Comparison of the predictions of literature intermolecular potentials for Ar–Xe and Kr–Xe with experiment: Two new potentials

R. A. Aziz and A. van Dalen

Citation: The Journal of Chemical Physics **78**, 2402 (1983); doi: 10.1063/1.445042
View online: http://dx.doi.org/10.1063/1.445042
View Table of Contents: http://scitation.aip.org/content/aip/journal/jcp/78/5?ver=pdfcov
Published by the AIP Publishing

Comparison of the predictions of literature intermolecular potentials for Ar–Xe and Kr–Xe with experiment: Two new potentials

R. A. Aziz and A. van Dalen

Guelph Waterloo Program for Graduate Work in Physics, Waterloo Campus, University of Waterloo, Waterloo, Ontario N2L 3G1, Canada
(Received 1 September 1982; accepted 17 November 1982)

Literature intermolecular potentials for the Ar–Xe and Kr–Xe systems are analyzed and critically assessed as to their abilities to predict dilute gas bulk and microscopic properties. Two new potentials of the HFD-C form (HFDAX1 and HFDKX1) are proposed for the Ar–Xe and Kr–Xe interactions, respectively, which accurately predict a large number of properties.

INTRODUCTION

Until recently, our knowledge of the Ar–Xe and Kr–Xe interactions has been much less satisfactory than for other mixed rare gas systems. First of all, let us consider the Ar–Xe interaction. Schaefer and Barker[1] derived a preliminary potential for Ar–Xe based on differential collision cross section (dccs) data. This potential predicts neither the total collision cross section (tccs) data of Linse *et al.*[2] nor the dilute bulk properties very well. The m-6-8 potential of Arora *et al.*[3] was fitted to dilute gas bulk data but its large epsilon and small r_m lead to poor scattering results. Maitland and Wakeham[4] used a semi-inversion procedure to develop a numerical potential from transport data but did not provide all the parameters necessary to express it in an analytical form. Barr *et al.*[5] used a similar procedure to invert new Ar–Xe viscosity data. They presented a numerical potential but no analytical form. On the basis of earlier tccs measurements, van den Biesen *et al.*[6] developed a Maitland–Smith potential. The potential gives a good description of new tccs data[7] apart from the glory amplitudes at $N=3$ and $N=4$. This potential, however, does not give, as we shall see, a good account of dccs scattering data[8] or dilute bulk data.

For the Kr–Xe system, three potentials were originally proposed. The first (LHB) due to Lee *et al.*[9] was developed from liquid phase properties. Using the Barker–Henderson perturbation theory, they calculated the excess free energy and excess volume for an equimolar liquid mixture at zero pressure at some specified temperature. They adjusted parameters in a potential of the Barker form until agreement with experiment was reached. The second potential was determined by Maitland and Wakeham[4] in numerical form by direct inversion of dilute gas transport data. This numerical potential was reexpressed in an analytical form of the Maitland–Smith type. The third potential for Kr–Xe was developed by van den Biesen *et al.*[6] on the basis of earlier tccs data.

As we shall see later, by far the best representation of the interaction for the Ar–Xe and Kr–Xe systems to date, are the potentials of Pack *et al.*[8] They fit a triple Morse–Spline–van der Waals functions (M3SV) to their dccs data, the virial data of Brewer[10] and Schramm and co-workers,[11,12] and the mixture viscosity data of Kestin *et al.*[13] We shall also see that the diffusion data of van Heijningen *et al.*[14] for both Ar–Xe and Kr–Xe and the Ar–Xe diffusion data of Arora *et al.*[3] are not quite predicted to within experimental error. Moreover, if the virial data of Brewer are revised in a way described below, the agreement between the predictions of the Ar–Xe potential with experiment is somewhat worsened. The virial results for Kr–Xe are still within experimental error, but the rms deviation is increased.

One purpose of this paper is to compare predictions of the various potentials mentioned above with a body of experimental data, both macroscopic and microscopic. Included in that body of data are the diffusion results of Arora *et al.*[3] and the new tccs data of van den Biesen.[7] The other purpose is to introduce two new potentials of the simpler HFD-C type which remove some of the minor difficulties associated with the M3SV potentials mentioned above. The HFD-C form has previously and successfully been applied to Ar–Ar, Ar–Kr, and Kr–Kr systems by Aziz and co-workers.[15–17]

THE DATA

Virial data

Brewer[10] measured "excess" virials for all binary noble gas mixtures including Ar–Xe and Kr–Xe. The interaction virial is obtained from the excess virial E_B and a knowledge of the second virial coefficients of the pure systems as follows:

$$B_{12} = E_B + 1/2(B_{11} + B_{22}) \ .$$

The excess virial can be measured more accurately for mixed systems than the second virial coefficient for a pure system. For the former, Brewer optimistically claimed an accuracy of 0.1 cc/mol. One can argue that the second virial for the pure systems calculated on the basis of accurate intermolecular potentials would be more reliable than experimental measurements especially where the potentials reliably predict spectroscopic and tccs data. These latter data accurately define the well of the potential and its long range tail. For argon and krypton, experimental and calculated values[15,17] agree well. For most temperatures, the deviations are less than 0.3 cc/mol and never more than 0.5 cc/mol. For xenon, the situation is rather different. The devia-

 0021-9606/83/052402-11$2.10

TABLE I. Parameters[a] for HFD–C Ar–Xe and Kr–Xe potentials.

	Ar–Xe (HFDAX1)	Kr–Xe (HFDKX1)
A^*	0.131 303 0(10)	0.141 690 6(10)
α^*	21.673 09	21.763 544
c_6	1.131 276 6	1.163 831 3
c_8	0.572 237 3	0.551 554 1
c_{10}	0.373 785 3	0.315 381 3
c_6 (a.u.)	139.223	207.237
c_8 (a.u.)	4159.30	6110.39
C_{10} (a.u.)	160 461.3	217 379.9
γ	5.35	5.40
D	1.566	1.550
ϵ/k (K)	188.63	233.48
r_m (Å)	4.0668	4.174
σ(Å)	3.645_4	3.740_8
B	3085.431 74	3124.255 86
β	3.687 470 17	3.744 861 18
x_0	0.353	0.3551

[a]Note: Not all figures displayed are significant. We display them only to avoid round off errors.

tion between experimental values used by Brewer and calculated values based on the accurate X4 potential of Barker *et al.*[18] is 6.7 cc/mol at 173.15 K, 3.1 cc/mol at 198.15 K, and 1.2 cc/mol at 223.15 K. For higher temperatures the agreement is better. It would, then, seem appropriate to revise the interaction virials using Brewer's excess virials and calculated $B(T)$ values for the pure systems.

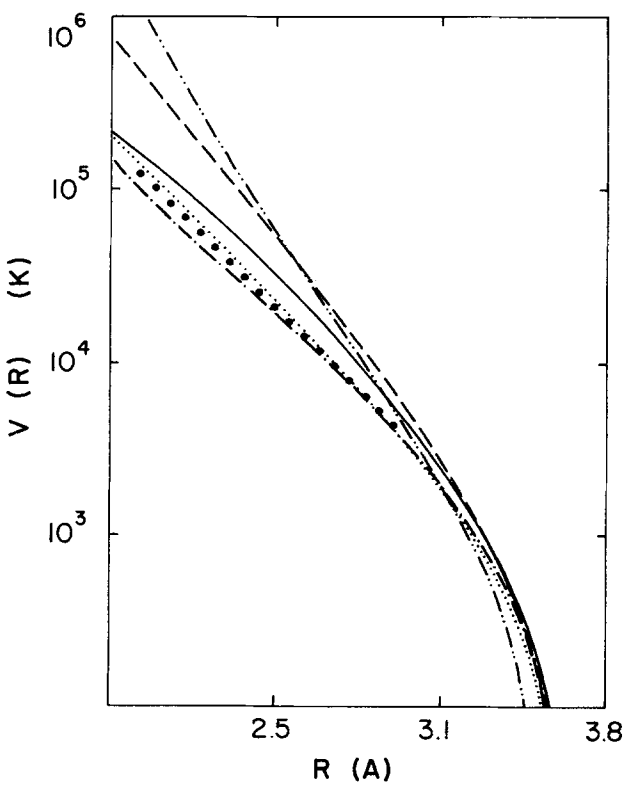

FIG. 1. Repulsive walls of Ar–Xe potentials: — HFDAX1; – – PACKAX; –•••– m68AX; –•–•–, SB; •••, MSVBAX; ●●●, RoI (Ref. 23).

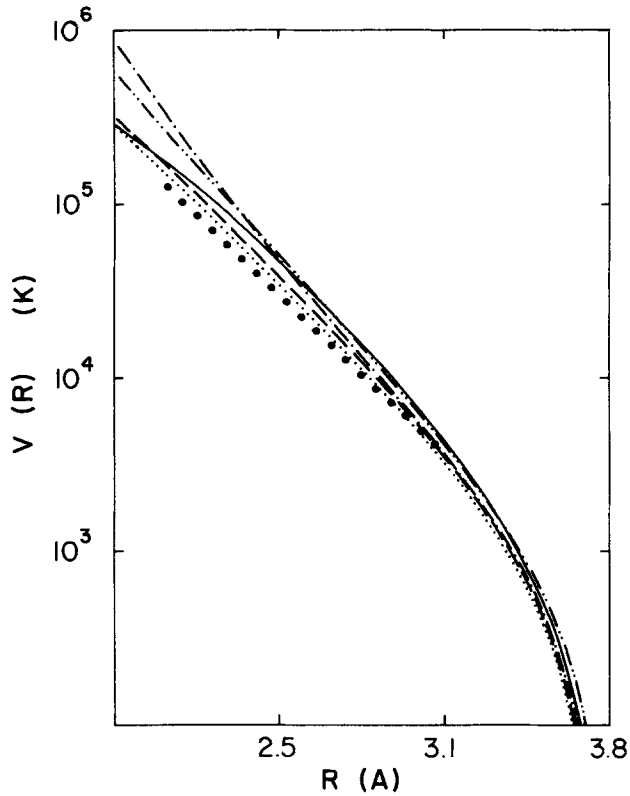

FIG. 2. Repulsive walls of Kr–Xe potentials: — HFDKX1; – – PACKKX; –••–••–, MW; –•–•–, LHB, •••, MSVBKX; ●●●, RoI (Ref. 23).

Also included in the analysis are the data of Schramm and co-workers[11,12] for which error bars of ±6 cc/mol are assigned and the second virial correlation of Kestin *et al.*[13]

Viscosity data

Interaction viscosity coefficients have been presented for Ar–Xe and Kr–Xe by Kestin *et al.*[13] for the temperature range 280–773 K. Mixture viscosities η_{12} were measured to better than ±0.5% and the procedure for extraction of the interaction viscosities with the aid of first-order kinetic theory introduced an additional error of approximately ±0.5%. Therefore, the total error assigned to η_{12} is ±1.0%.

Diffusion data

For the Ar–Xe system, three sets of diffusion data are employed in our analysis. First, van Heijningen *et al.*,[14] using a two-chamber cell, have measured the diffusion coefficient D_{12}, in the temperature region 169–400 K. Second, Hogervorst,[19] using a cataphoresis technique, has measured diffusion coefficients for Ar–Xe over a temperature range of 300–1400 K. Both sets of data are quoted to an accuracy of ±1.0%. Finally, Arora *et al.*[3] presented very precise diffusion coeffi-

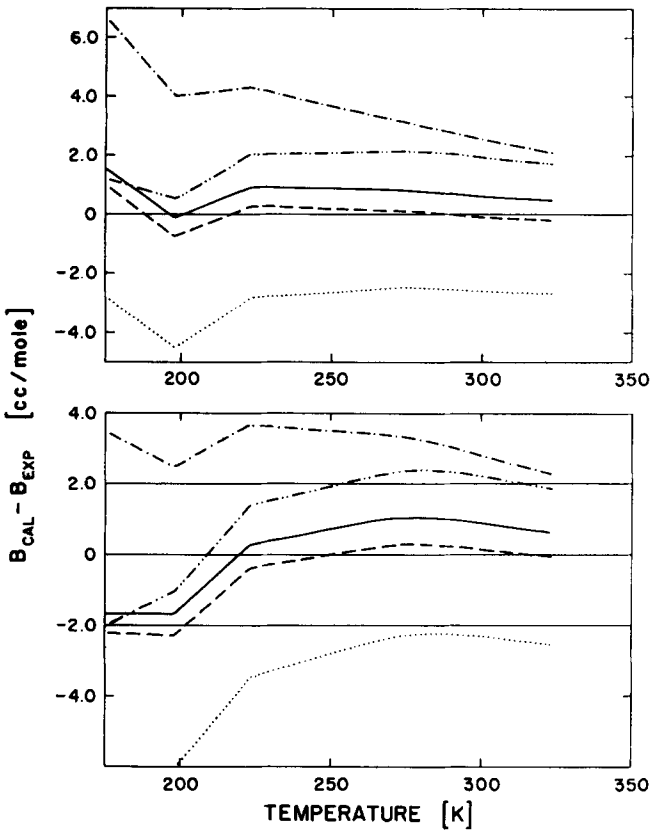

FIG. 3. Deviation plots for Ar–Xe second virial coefficients. Upper plot: original brewer data; lower plot; revised Brewer data. Legend as in Fig. 1.

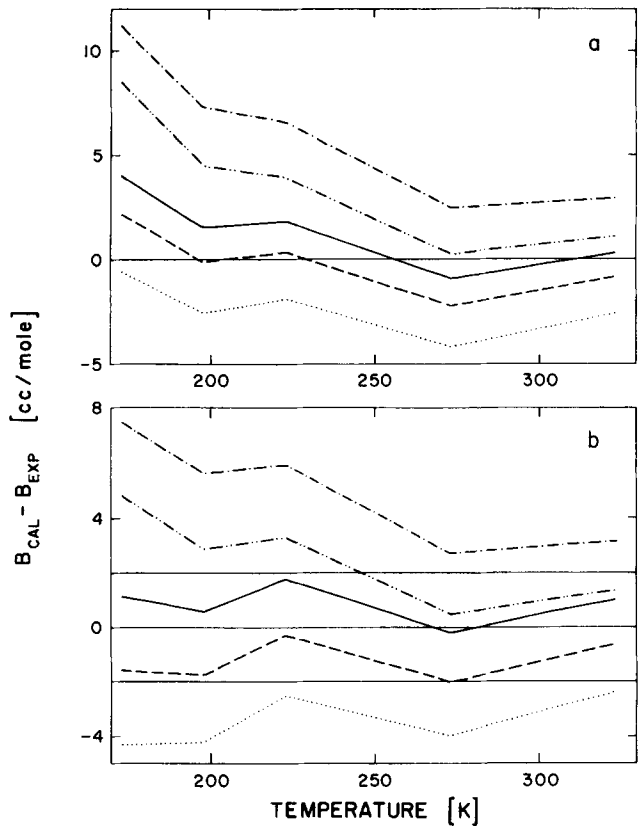

FIG. 5. Deviation plots for Kr–Xe second virial coefficients. Upper plot: original brewer data; lower plot: revised Brewer data. Legend as in Fig. 2.

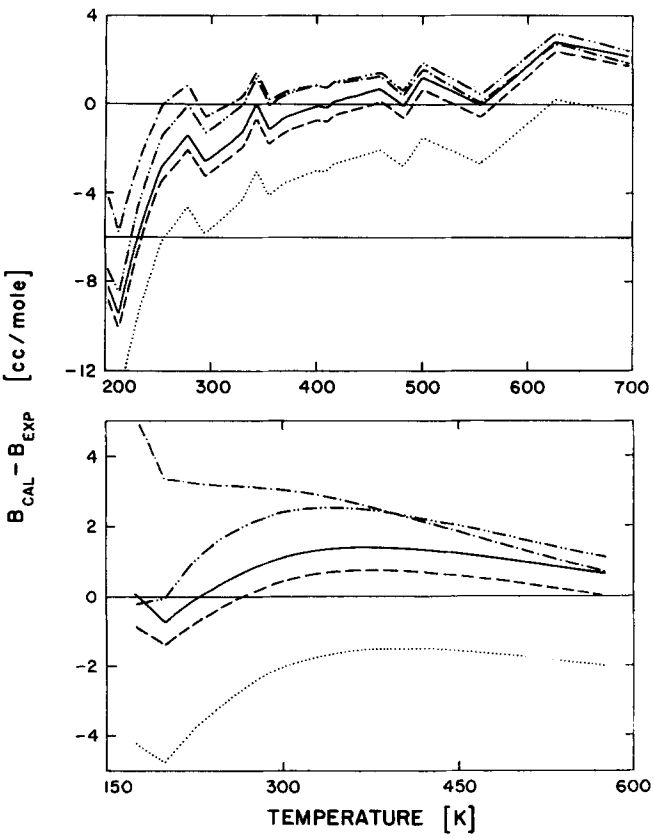

FIG. 4. Deviation plots for Ar–Xe second virial coefficients. Upper plot: Schramm and co-workers data; lower plot: Kestin *et al.* (Ref. 13) data. Legend as in Fig. 1.

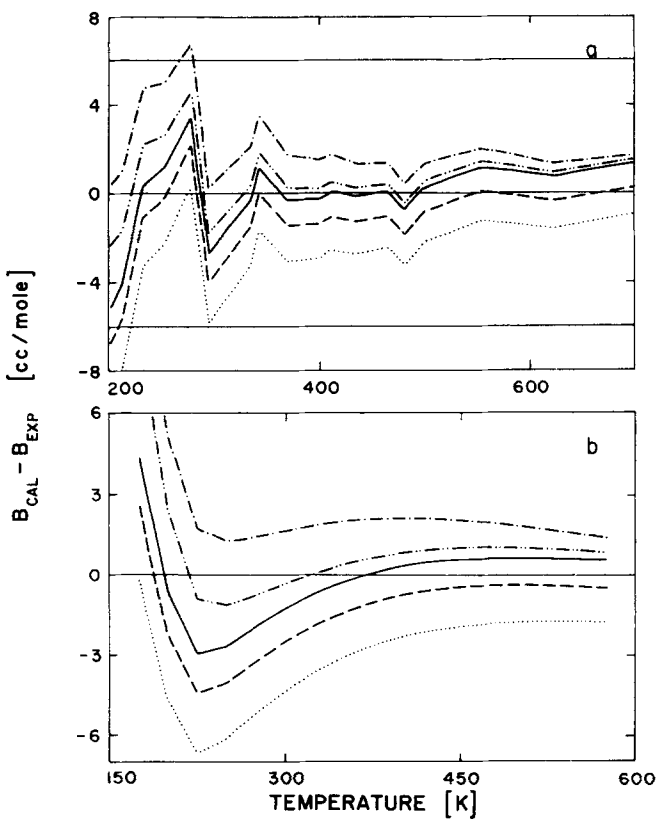

FIG. 6. Deviation plots for Kr–Xe second virial coefficients. Upper plot: Schramm and co-workers data; Lower plot: Kestin *et al.* (Ref. 13) data. Legend as in Fig. 2.

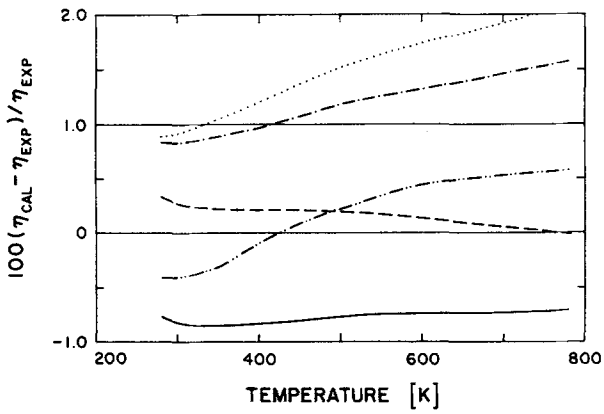

FIG. 7. Deviation plots for Ar–Xe interaction viscosity. Data of Kestin *et al.* (Ref. 13). Legend as in Fig. 1.

cients for Ar–Xe over a temperature interval from 277 to 323 K. Accuracy for these latter data are given as ±0.1%. While this value appears optimistic, previous work on He–Ar[20] and Ar–Kr[16] seems to substantiate the estimate. The only reliable data available for the Kr–Xe system are those of van Heijningen *et al.*

Total collision cross sections

van den Biesen *et al.*[6] measured total cross section data for Ar–Xe over the relative velocity range 650–3500 m/s and for Kr–Xe over the range 500–4000 m/s. Recently, refinements in the apparatus were made by van den Biesen[7] and more precise tccs data are presented for Ar–Xe(637–3709 m/s), Xe–Ar(870–3260 m/s), Kr–Xe(490–3280 m/s), and Xe–Kr(797–1300 m/s). These latter data are analyzed in this paper.

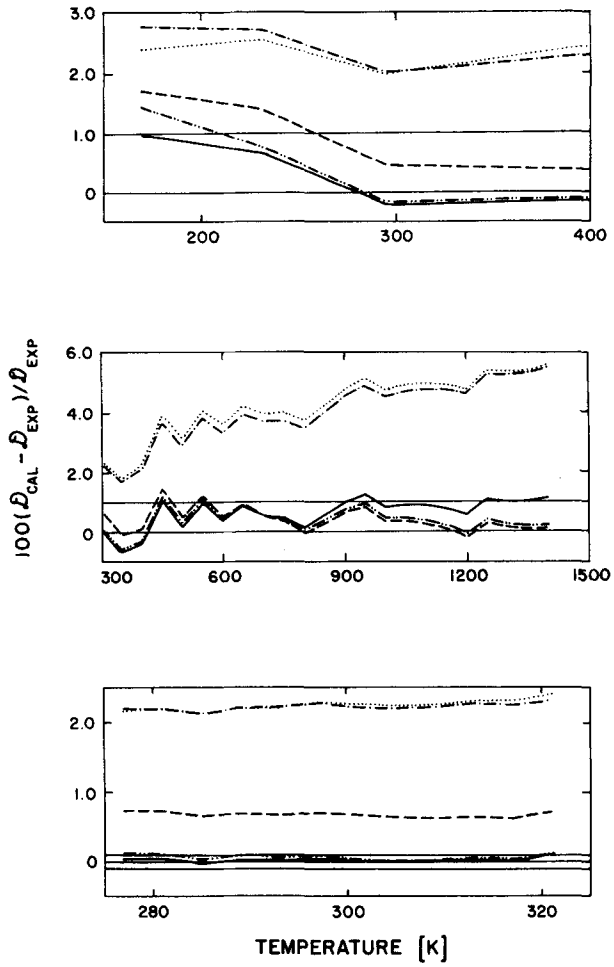

FIG. 9. Deviation plots for the Ar–Xe diffusion coefficient. Upper plot-Data of van Heijningen *et al.* (Ref. 14). Middle plot-Data of Hogervorst (Ref. 19). Lower plot-Data of Arora *et al.* (Ref. 3). Legend as in Fig. 1.

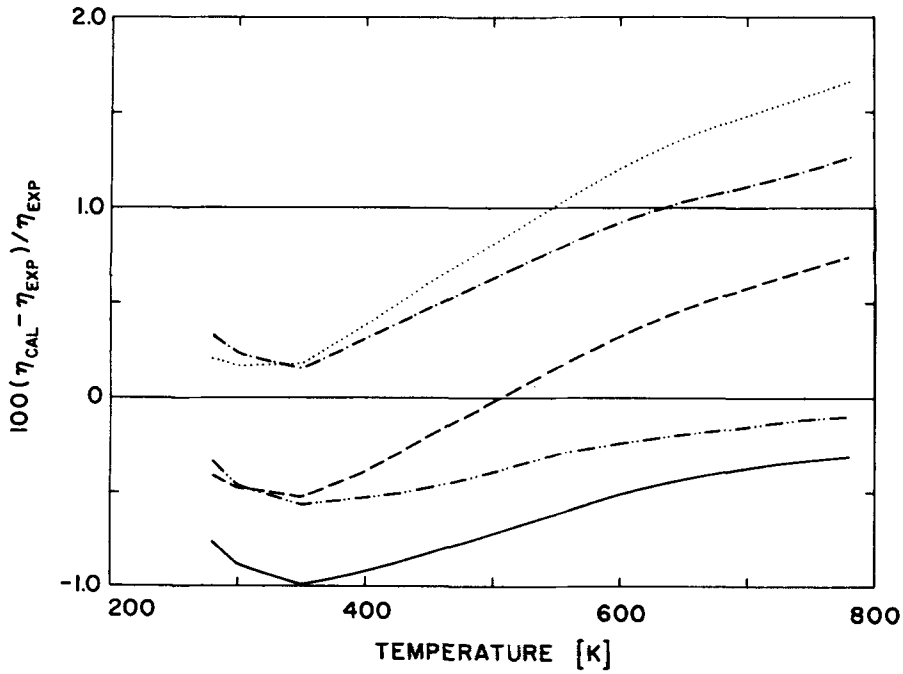

FIG. 8. Deviation plots for Kr–Xe interaction viscosity. Data of Kestin *et al.* (Ref. 13). Legend as in Fig. 2.

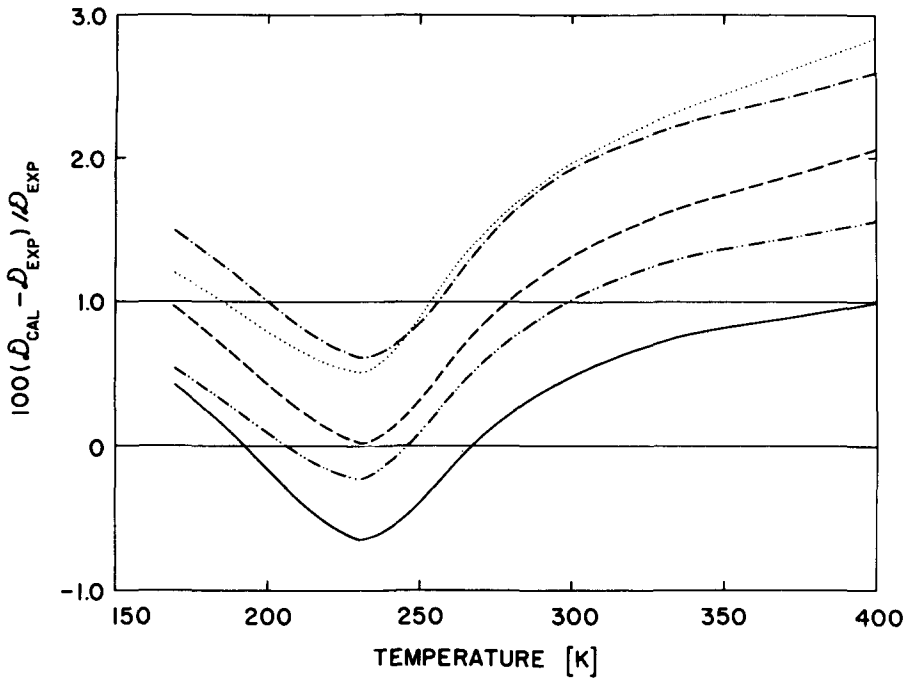

FIG. 10. Deviation plots for the Kr–Xe diffusion coefficient. Data of van Heijningen *et al.* (Ref. 14). Legend as in Fig. 2.

Differential collision cross sections

Cross molecular beam measurements for the scattering of Ar and Kr by Xe were reported by Pack *et al.*[8] The relative energy is approximately 741 K for both cases.

The potentials

The HFD-C potential is a modification by Aziz and co-workers[15–17] of the HFD potential first introduced by Ahlrichs *et al.*[21] The latter potential has no adjustable parameters and uses an input self-consistent-field Hartree–Fock repulsion between closed shell systems when available, a semiempirical estimate of the correlation energy and semiempirically determined dispersion coefficients.

The form of the modified HFD-C potential is

$$V(r) = \epsilon V^*(x) ,$$

$$V^*(x) = A^* x^{\gamma} \exp(-\alpha^* x) - (c_6/x^6 + c_8/x^8 + c_{10}/x^{10}) F(x) ,$$

where

$$F(x) = \exp[-(D/x - 1)^2] \quad \text{for } x < D ,$$

$$= 1 \quad \text{for } x > D ,$$

and

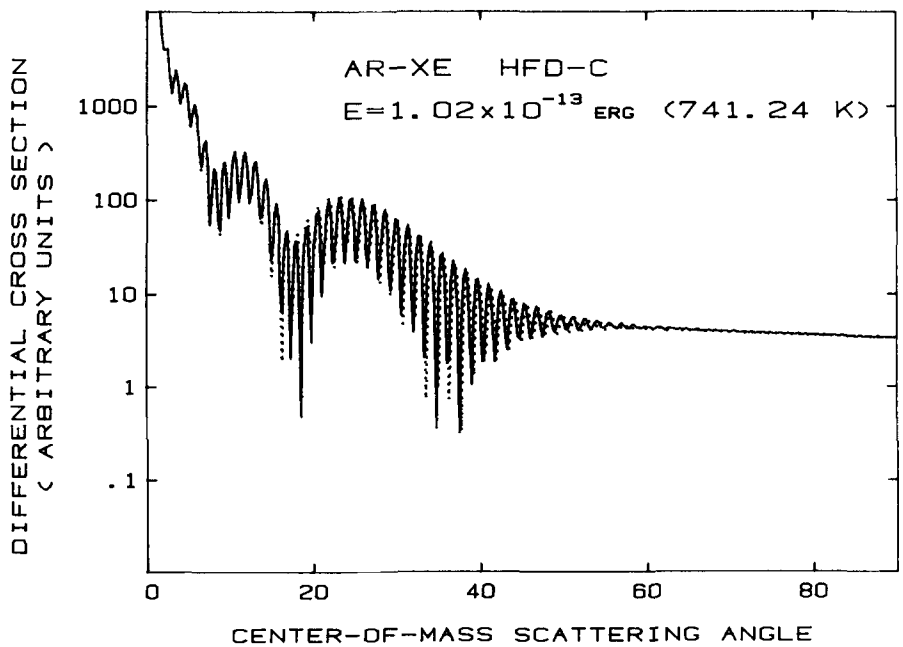

FIG. 11. Differential cross sections (Ar–Xe) for the energy of $E = 741.2$ K in the center of mass frame of reference calculated for the HFDAX1 potential (solid line) compared with that calculated for the PACKAX potential (dots).

TABLE II. Ar–Xe, rms deviations for various potentials.

		Parameters			Property[a]						
Potential	Reference	ϵ/k (A)	r_m (K)	τ	B^b $cm^3\,mol^{-1}$	B^c $cm^3\,mol^{-1}$	B^d $cm^3\,mol^{-1}$	η^e μP	D^f $cm^2\,s^{-1}$	D^g $cm^2\,s^{-1}$	D^h $cm^2\,s^{-1}$
HFDAX1	Present	188.63	4.0668	3.645_4	1.184	3.27	1.03	2.66(0.78)	0.0086(0.79)	0.0003(0.60)	0.0000(0.04)
PACKAX	Pack *et al.* (1982)	188.84	4.038	3.623	1.439	3.59	0.63	0.49(0.18)	0.0030(0.57)	0.0007(1.15)	0.0008(0.67)
SB	Schaefer &Barker[i]	185.0	4.063	3.625	3.094	1.94	2.68	4.63(1.21)	0.0457(4.15)	0.0027(2.46)	0.0025(2.22)
MSVBAX	van den Biesen *et al.* (1980).	187.4	4.06	3.615	4.393	5.51	2.48	6.04(1.55)	0.0471(4.34)	0.0028(2.35)	0.0026(2.25)
m68AX	Arora *et al.* (1979)	212.5	3.9451	3.558	1.793	2.90	1.87	1.55(0.40)	0.0036(0.55)	0.0004(0.82)	0.0001(0.07)

[a]Quantities refer to root-mean-squared deviations and quantities in parentheses refer to root-mean-squared *percentage* deviation.
[b]Brewer (Ref. 10) virials (revised: see the text).
[c]Schramm *et al.* (Refs. 11 and 12) virials. Estimated error ±6.0 $cm^3\,mol^{-1}$.
[d]Kestin *et al.* (Ref. 13) virials.
[e]Kestin *et al.* (Ref. 13) interaction viscosity. Estimated error ±1%.
[f]Hogervorst (Ref. 19) diffusion. Estimated error ±1%.
[g]van Heijningen *et al.* (Ref. 14) diffusion. Estimated error ±1%.
[h]Arora *et al.* (Ref. 3) diffusion. Estimated error ±0.1%.
[i]As cited in Bobetic and Barker (Ref. 1).

$$c_n = C_n/(\epsilon r_m^n) .$$

In our fitting procedure, C_6, C_8, C_{10} are all normally held within the bounds given by Tang *et al.*[22] (However, systems involving xenon appear to have dispersion coefficients which lie on the low side.[7]) Parameters γ, D, ϵ, and r_m are also allowed to vary while A^* and α^* are determined by the conditions imposed on the potential at its minimum viz., $V^*(1) = -1$ and $dV^*(1)/dx = 0$. The properties chosen for the fit are the revised second virial coefficients of Brewer,[10] the interaction viscosity of Kestin *et al.*[13] and the low temperature diffusion coefficients of van Heijningen[14] and the room temperature diffusion coefficients of Arora *et al.*[3] when available.

Potentials for these systems required large values of the parameter γ and as a result the potentials turn over. To ensure that the repulsive wall possesses a negative slope to very small separations, a function of the form

$$B\exp(-\beta x)/x$$

is smoothly connected to $V^*(x)$ at x_0 for the region $x \leq x_0$. This should not pose any serious problem since no physical observable senses the potential at separations of the order of x_0 or less.

Parameters for the HFD-C (HFDAX1 and HFDKX1) potentials are given in Table I.

RESULTS AND DISCUSSION

In Fig. 1, the five repulsive walls of the Ar–Xe potentials are plotted (m68AX, SB, MSVBAX, PACKAX, and HFDAX1) together with that proposed by Rol[23] which was fitted to his high energy total cross sections. The MSVBAX and SB potentials are in closest agreement with that of Rol. While the HFDAX1 potential lies above that of Rol, the PACKAX potential is by far the hardest.

The repulsive walls of the Kr–Xe potentials are plotted in Fig. 2. All potentials have roughly similar repulsive walls, lying somewhat above that of Rol. The MSVBKX potential is closest to and the HFDKX1 is farthest from it.

Because of an apparent inflexibility of the HFD-C form, closer agreement with Rol's potential could not be achieved.

Second virial coefficients

Second virial coefficients were calculated for all potentials. The first and second quantum corrections were included even though the latter was negligible for all but the lowest temperatures.

The deviation plots for the Ar–Xe data of Brewer are given in Fig. 3 (upper: original data; lower: revised data). The HFDAX1 potential was fitted to the revised data and hence lies within the error bands of ±2 cc/mol. As mentioned above, the PACKAX potential which was fitted to the original data gives predictions which lie just outside the error bounds for the lowest two temperatures. The deviation plots for the Ar–Xe data of Schramm and co-workers[11,12] are shown in Fig. 4

TABLE III. Kr–Xe, rms deviations for various potentials.

		Parameters			Property[a]				
Potential	Reference	ϵ/k (K)	r_m (Å)	σ (Å)	B[b] $cm^3\,mol^{-1}$	B[c] $cm^3\,mol^{-1}$	B[d] $cm^3\,mol^{-1}$	η[e] μP	D[f] $cm^2\,s^{-1}$
HFDKX1	Present	233.48	4.174	3.740_8	1.078	1.976	1.607	2.33(0.68)	0.0007(0.68)
PACKKX	Pack *et al.* (1982)	231.46	4.191	3.738_2	1.415	2.514	2.068	2.05(0.46)	0.0014(1.30)
MW	Maitland & Wakeham (1978)	220	4.230	3.771	2.967	1.735	2.316	1.19(0.36)	0.0011(0.96)
LHB	Lee *et al.* (1975)	228.92	4.1786	3.7298	5.278	2.725	3.443	3.84(0.80)	0.0019(1.79)
MSVBKX	van den Biesen *et al.* (1980)	231.1	4.18	3.720	3.577	3.872	3.506	5.03(1.04)	0.0020(1.82)

[a]Quantities refer to root-mean-squared deviations, and quantities in parentheses refer to root-mean-squared *percentage* deviations.
[b]Brewer (Ref. 10) virials (revised: see the text).
[c]Schramm *et al.* (Refs. 11 and 12) virials. Estimated error ±6.0 $cm^3\,mol^{-1}$.
[d]Kestin *et al.* (Ref. 13) virials.
[e]Kestin *et al.* (Ref. 13) interaction viscosity. Estimated error ±1%.
[f]van Heijningen *et al.* (Ref. 14) diffusion. Estimated error ±1%.

(upper). As Barr *et al.*[5] points out, the data at the lowest two temperatures seems to have errors which exceed those quoted viz., ±6 cc/mol. When these two points are neglected, all but the MSVBAX potential give predictions within these bounds for the rest of the temperature range. For completeness the deviation plots for the second virial coefficient correlation of Kestin *et al.* is shown in Fig. 4 (lower).

The deviation plots for the corresponding data for Kr–Xe are given in Fig. 5 (upper: original Brewer data; lower: revised Brewer data) and in Fig. 6 (upper: Schramm and co-workers data; lower: Kestin *et al.* data). Only the HFDKX1 and PACKKX potentials give predictions which lie within the ±2 cc/mol error bounds of Brewer's revised data. Not surprisingly, the data of Schramm and co-workers with associated large error bounds of ±6 cc/mol are predicted by almost all potentials. The MSVBKX potential does not predict the lowest two temperatures. Again for completeness we include the data of Kestin *et al.*

Transport data

The interaction viscosity coefficient η_{12} are calculated in the third-order Chapman–Cowling approximation employing classical collision integrals computed with a program developed by O'Hara and Smith[24] and adapted for use on IBM computers.[25] The diffusion coefficients D_{12} are determined in a three potential calculation employing Chapman–Cowling relations to give the composition dependence (Sec. 2.4 of Ref. 26). The poten-

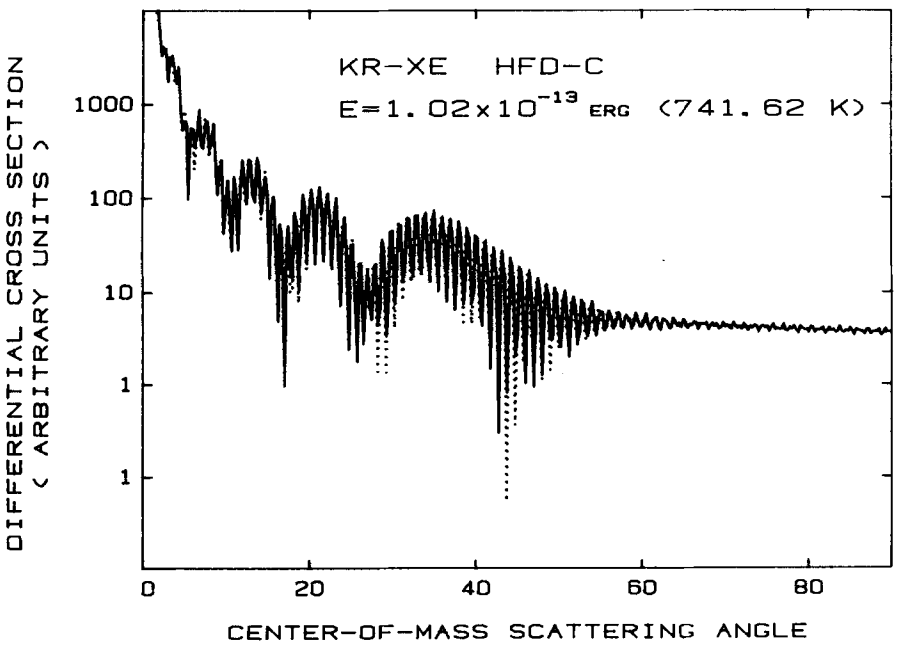

FIG. 12. Differential cross sections (Kr–Xe) for the energy of $E = 741.62$ K in the center of mass frame of reference calculated for the HFDKX1 potential (solid line) compared with that calculated for the PACKKX potential (dots).

TABLE IV. Ar–Xe, rms deviations for various potentials.

		Microscopic property		
		$I(\theta)$[a]	$Q(\bar{g})$[b]	$Q(\bar{g})$[c]
Potential	Reference	$T=741.24$ K	Ar–Xe	Xe–Ar
HFDAX1	Present	0.159	0.004 06	0.005 51
PACKAX	Pack *et al.*[e]	standard	0.005 54	0.006 16
SB	Schaefer and Barker[d]	0.082	0.015 69	0.014 07
MSVBAX	van den Biesen *et al.*[f]	0.061	0.004 08	0.005 70
m68AX	Arora *et al.*[g]	0.457	0.027 27	0.024 38

[a]Pack *et al.* (Ref. 8) differential cross sections.
[b]van den Biesen *et al.* (Ref. 7) total cross sections (Ar–Xe).
[c]van den Biesen *et al.* (Ref. 7) total cross sections (Xe–Ar).
[d]As cited in Bobetic and Barker (Ref. 1).
[e]Reference 8.
[f]Reference 6.
[g]Reference 3.

TABLE V. Kr–Xe, rms deviations for various potentials.

		Microscopic property		
		$I(\theta)$[a]	$Q(\bar{g})$[b]	$Q(\bar{g})$[c]
Potential	Reference	$T=741.62$ K	Kr–Xe	Xe–Kr
HFDKX1	Present	0.094	0.003 94	0.003 71
PACKKX	Pack *et al.*[d]	standard	0.004 74	0.004 98
MW	Matiland and Wakeham[e]	0.366	0.017 49	0.015 34
LHB	Lee *et al.*[f]	0.158	0.015 46	0.011 06
MSVBKX	van den Biesen *et al.*[g]	0.153	0.003 90	0.003 88

[a]Pack *et al.* (Ref. 8) differential cross sections.
[b]van den Biesen *et al.* (Ref. 7) total cross sections (Kr–Xe).
[c]van den Biesen *et al.* (Ref. 7) total cross sections (Xe–Kr).
[d]Reference 8.
[e]Reference 4.
[f]Reference 9.
[g]Reference 6.

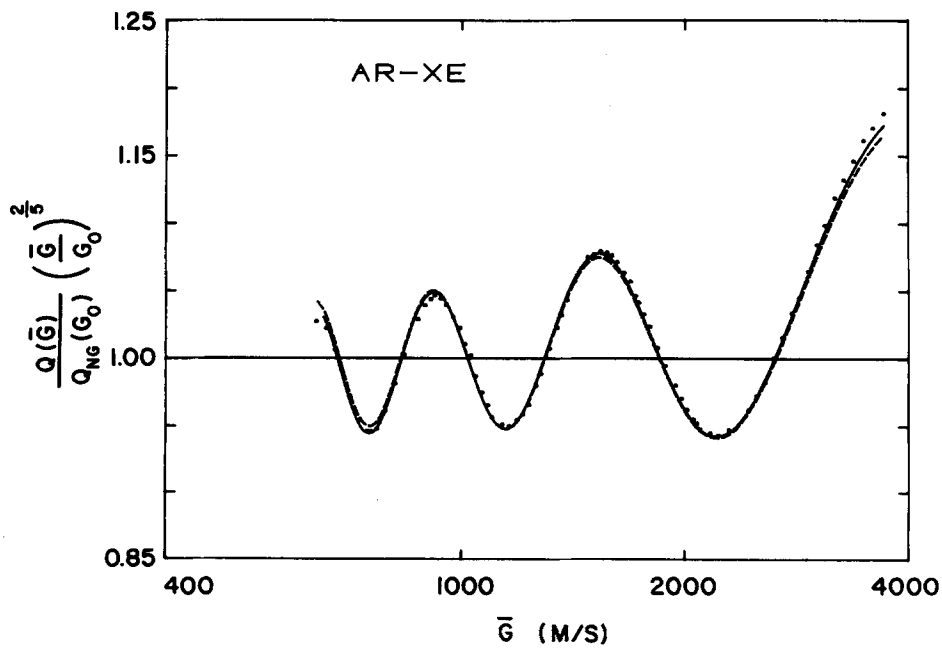

FIG. 13. Comparison of the experimental total cross section data of van den Biesen *et al.* (Ref. 7) (dots) with the total cross sections calculated on the basis of the present (HFDAX1) potential (solid line); PACKKX (dashed line): Ar (primary beam)—Xe (secondary beam).

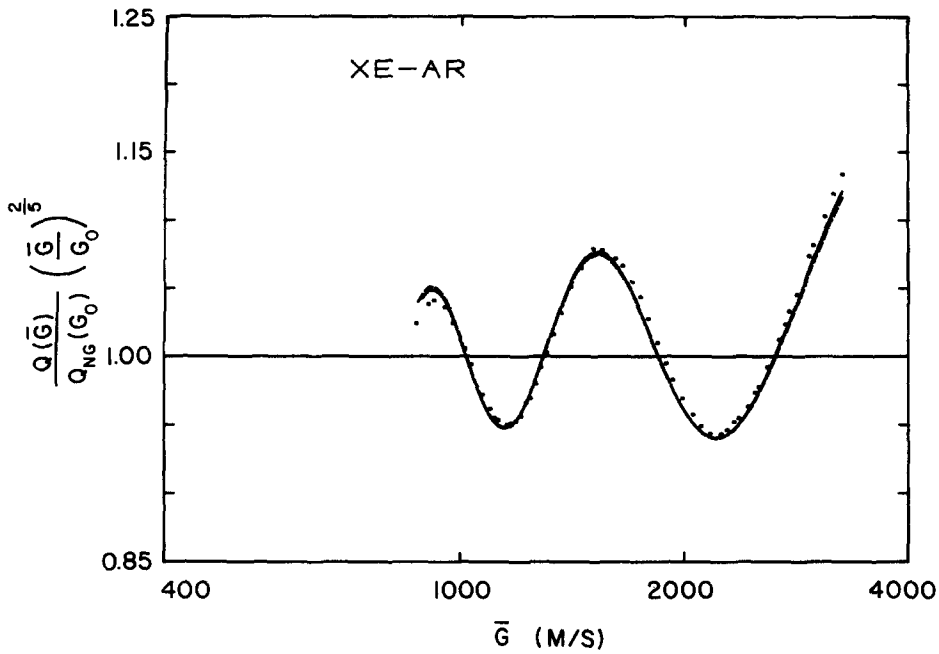

FIG. 14. Comparison of the experimental cross section data of van den Biesen *et al.* (Ref. 7) (dots) with the total cross sections calculated on the basis of the present (HFDAX1) potential (solid line); PACKAX (dashed line): Xe (primary beam)–Ar (secondary beam).

tials used for the Ar–Ar and Kr–Kr interactions are those of Aziz and co-workers.[15,17] The Xe–Xe potential is the X4 potential of Barker *et al.*[18]

Viscosity

The deviation plots for the Kestin *et al.* interaction viscosity data are given in Fig. 7. Not surprisingly, only the PACKAX, HFDAX1, and m68AX Ar–Xe potentials, which were fitted in part to the Brown University mixture or interaction viscosity data, all give predictions within the error bounds of ±1.0% for η_{12}.

For Kr–Xe, only the PACKKX, HFDKX1, and MW Kr–Xe potentials, which were fitted to the mixture or interaction viscosity, predict this property to within error limits. The deviation plots for these potentials are displayed in Fig. 8.

Diffusion

The deviation plots for the three sets of diffusion data are shown in Fig. 9. The HFDAX1 potential was fitted to the van Heijningen *et al.* (VH) and Arora *et al.* (DN) data but also predicts the Hogervorst (HG) data. The PACKAX potential predicts the HG data but not all of the VH or DN data to within experimental error. The m68AX potential was fitted to the DN and HG data but does not predict the VH data point at 169.3 K.

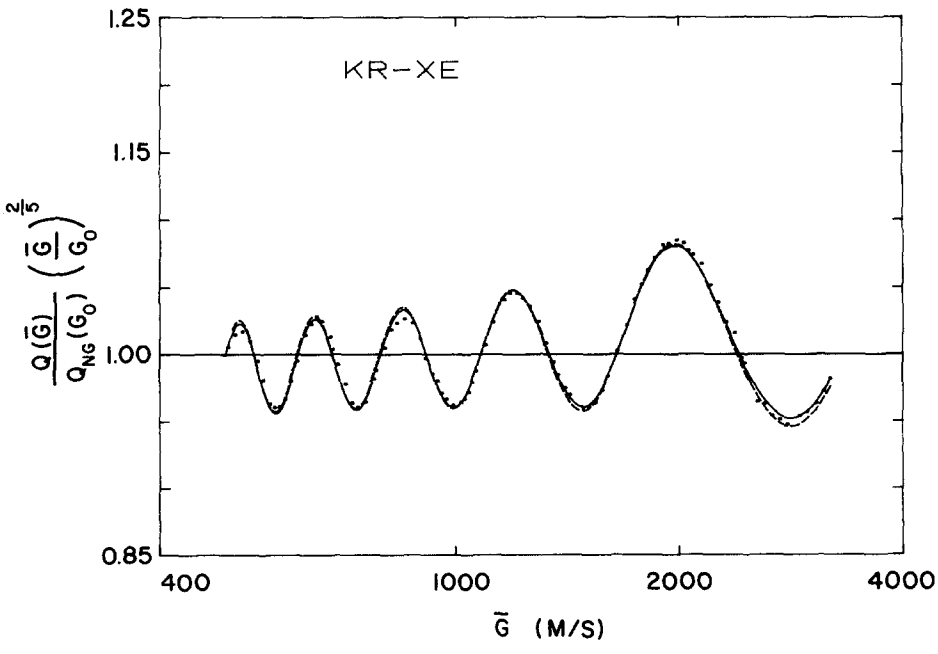

FIG. 15. Comparison of the experimental total cross section data of van den Biesen *et al.* (Ref. 7) (dots) with the total cross sections calculated on the basis of the present (HFDKX1) potential (solid line); PACKKX (dashed line): Kr (primary beam)–Xe (secondary beam).

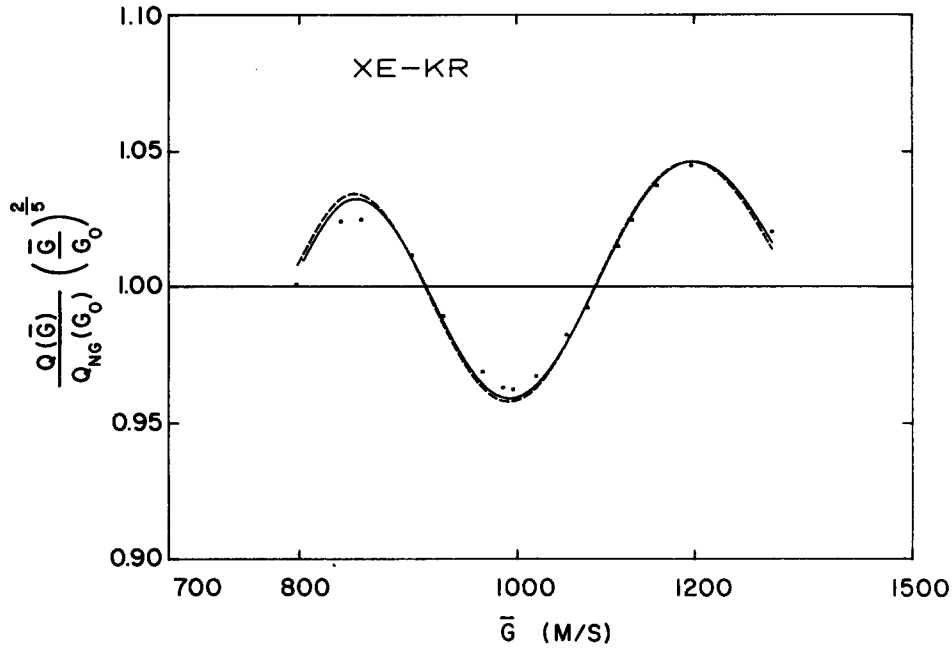

FIG. 16. Comparison of the experimental total cross section data of van den Biesen *et al.* (Ref. 7) (dots) with the total cross sections calculated on the basis of the present (HFDKX1) potential (solid line); PACKKX (dashed line): Xe (primary beam)–Kr (secondary beam).

Of all the Kr–Xe potentials considered, the HFDKX1 alone predicts the VH diffusion data. The deviation plots for Kr–Xe are shown in Fig. 10.

Rms deviations for second virial coefficient and transport properties are presented in Table II (Ar–Xe) and in Table III (Kr–Xe). Quantities in parentheses refer to root-mean-squared *percentage* deviations.

Differential cross sections

To assess the ability of the various potentials to predict dccs data, the following approach is taken. The Pack *et al.* potentials to which the original data was fitted were used to generate pseudo dccs in the center-of-mass frame of reference. These data generated in this way are considered as standard data with which the predictions based on other potentials may be compared. Resolution of the "experimental" pseudodata is infinite and consequently substantial structure in the cross section is evident. The results for the HFD-C potentials are presented in Figs. 11 and 12 where the dots represent the Pack *et al.* pseudodata and the continuous line is the prediction of the corresponding HFD-C potential. The agreement seems to be quite satisfactory. The rms deviations between the logarithms of the theoretical and pseudodata calculated at 0.25° intervals from 0° to 90° in the center-of-mass frame of reference is taken as a measure of the goodness of fit. The rms deviations for all of the potentials from the standard are presented in Table IV and Table V.

Total cross sections

Also presented in Table IV and Table V are the rms deviations between experimental and theoretical tccs on the basis of the various potentials for each of Ar (primary beam)–Xe (secondary beam), Xe (primary beam)–Ar (secondary beam), Kr (primary beam)–Xe (secondary beam), and Xe (primary beam)–Kr (secondary beam).

The Ar–Xe results for the HFDAX1 and PACKAX potentials are displayed in Figs. 13 and 14, and the Kr–Xe results for HFDKX1 and PACKKX potentials are presented in Figs. 15 and 16. In each case both sets of potentials provided an excellent account of the tccs data although the HFD-C potentials give noticeably better results especially at high relative velocities. The rms deviations (Table IV and Table V) for the HFD-C potentials are thus considerably smaller. The improvement is probably a result of a better long range in each case.

In conclusion, the Pack *et al.* and the present HFD-C potentials give an excellent representation of the Ar–Xe and Kr–Xe interaction. Insofar as dccs to which the Pack *et al.* potentials were fit, the former are superior. Insofar as the tccs, diffusion, and second virial data, the HFD-C potentials have the edge. Moreover the HFD-C potentials are simpler and probably more realistic in form.

ACKNOWLEDGMENT

This work was supported in part by the National Sciences and Engineering Research Council of Canada.

[1] M. V. Bobetic and J. A. Barker, J. Chem. Phys. **64**, 2367 (1976).
[2] C. A. Linse, J. J. H. van den Biesen, E. H. van Veen, and C. J. N. van den Meijdenberg, Physica (Utrecht) **99**, 166 (1979).
[3] P. S. Arora, H. L. Robjohns, and P. J. Dunlop, Physica (Utrecht) **95**, 561 (1979).
[4] G. C. Maitland and W. A. Wakeham, Mol. Phys. **35**, 1443 (1978).
[5] I. A. Barr, G. P. Matthews, E. B. Smith, and A. R. Tindell, J. Phys. Chem. **85**, 3342 (1981).
[6] J. J. H. van den Biesen, F. A. Stokvis, E. H. van Veen, and C. J. N. van den Meijdenberg, Physica (Utrecht) **100**, 375 (1980).

[7]J. J. van den Biesen, R. M. Hermans, and C. J. N. van den Meijdenberg, Physica Status Solidi A **115**, 396 (1982).
[8]R. T Pack, J. J. Valentini, C. H. Becker, R. J. Buss, and Y. T. Lee, J. Chem. Phys. **77**, 5475 (1982).
[9]J. K. Lee, D. Henderson, and J. A. Barker, Mol. Phys. **29**, 429 (1975).
[10]J. Brewer, Tech. Rept. AD663448, AFOSR Contract No. AF49(638)-1620 (1967). Available from the Clearinghouse for Federal Scientific and Technical Information.
[11]B. Schramm, H. Schmiedel, R. Gerhmann, and R. Bartl, Ber. Bunsenges. Phys. Chem. **81**, 316 (1977).
[12]H. P. Rentschler and B. Schramm, Ber. Bunsenges. Phys. Chem. **81**, 319 (1977).
[13]J. Kestin, H. E. Khalifa, and W. A. Wakeham, Physica (Utrecht) **90**, 215 (1978).
[14]R. J. J. van Heijningen, J. P. Harpe, and J. J. M. Beenakker, Physica (Utrecht) **38**, 1 (1968).
[15]R. A. Aziz and H. H. Chen, J. Chem. Phys. **67**, 5719 (1977).
[16]R. A. Aziz, J. Chem. Phys. (to be published).
[17]R. A. Aziz, Mol. Phys. **38**, 177 (1979).
[18]J. A. Barker, M. L. Klein, and M. V. Bobetic, IBM J. Res. Dev. **20**, 222 (1976).
[19]W. Hogervorst, Physica (Utrecht) **51**, 59 (1971).
[20]R. A. Aziz, P. W. Riley, U. Buck, G. Maneke, J. Schleusener, G. Scoles, and U. Valbusa, J. Chem. Phys. **71**, 2637 (1979).
[21]R. Ahlrichs, P. Penco, and G. Scoles, Chem. Phys. **19**, 119 (1976).
[22]K. T. Tang, J. M. Norbeck, and P. R. Certain, J. Chem. Phys. **64**, 3063 (1976).
[23]P. Rol (private communication).
[24]H. Smith and F. J. O'Hara, Comput. Phys. Commun. **2**, 47 (1971).
[25]P. D. Neufeld and R. A. Aziz, Comput. Phys. Commun. **3**, 269 (1972).
[26]T. R. Marrero and E. A. Mason, J. Phys. Chem. Ref. Data **1**, 3 (1972).